Optimal power flow with distributed energy storage dynamics

Dennice Gayme and Ufuk Topcu

Abstract— **Restructuring of the electric power industry along with mandates to integrate renewable energy sources is introducing new challenges for electric power systems and the power grid. Intermittent power sources in particular require mitigation strategies in order to maintain consistent power on the electric grid. We investigate distributed energy storage as one such strategy. Our model for optimal power flow consists of simple charge/discharge dynamics for energy storage collocated with load and/or generation buses cast as a finite-time optimal control problem. We illustrate the effects of energy storage using a modified version of the IEEE 14 bus benchmark example along with time-varying demand profiles. We use both time-invariant and demand based cost functions. The addition of energy storage along with demand based cost functions significantly reduces the generation costs and flattens the generation profiles.**

I. Introduction

Electric power systems and the power grid are currently undergoing a restructuring due to a number of factors such as; increasing demand, increasing uncertainty caused by the integration of intermittent renewable energy sources, and further deregulation of the industry [1], [2], [3]. The integration of renewables in particular is being accelerated by government mandates, e.g., see [4] which details these directives for 30 US states. The operational challenges associated with these trends can be alleviated by effectively utilizing grid-integrated distributed energy storage [5]. The potential benefits of grid-integrated storage technologies include decreasing the need for new transmission or generation capacity, improving load following, providing spinning reserve, correcting frequency, voltage, and power factors, as well as the indirect environmental benefits of facilitating the integration of nonpolluting, renewable energy sources [6]. Although the benefits of such storage schemes are widely accepted, the appropriate storage technology along with the required capacity and rates of charge/discharge are a continuing research topic [7]. Criteria for an effective storage strategy include (i) dispatchability – response to fluctuations in electricity demand; (ii) interruptibility – reaction to the intermittency in energy supplies like wind and solar; and (iii) efficiency – recovering energy that is otherwise wasted [8].

The promise of effective grid-integrated energy storage has led to considerable research activity. The role of storage in power regulation and peak-shaving was studied through simulation as early as 1981 [9]. More recently, the utility of energy storage in mitigating the effects of integrating renewable resources into the power grid has been investigated in both the traditional [10], [11] and micro-grid [12] settings. Efficiency of energy storage allocation in terms of minimizing curtailed wind energy (in a system with a high penetration of wind generation) was addressed by the authors of [13]. The question of interruptibility (probability of load-shedding) has also been investigated through the use of different combinations of hybrid generation (i.e., a combination of wind, solar and fossil fuel based generation systems) versus storage capacities, in the special case of an isolated system [14].

The optimal power flow (OPF) problem [15], [16], [17], [18] optimizes some cost function, e.g., generation cost and/or user utilities, over variables such as; real and reactive power outputs, voltages, and phase angles at a number of buses subject to, capacity and network constraints. It has been extensively studied since the work of Carpentier [19]. The surveys in [20], [21], [22] provide a historical overview of special instances of the problem and various solution strategies. More recent work attempted to reformulate the problem into more tractable realizations. For example, references [23], [24] considered radial distribution systems as conic programming problems and [25] proposed a convex relaxation that is equivalent to the OPF problem under certain conditions (discussed later in this paper).

The formulation in this paper extends the OPF problem formulation in [25] to integrate simple charge/discharge dynamics of energy storage distributed over the network. The inclusion of these energy storage dynamics leads to a finite-horizon optimal control problem that enables optimization of (dynamic) power allocation over time in addition to the static allocation over the network. The current formulation augments the ideas presented in [26] through elimination of the small-angle assumption and the addition of power rate limits on the energy storage. The expanded problem setting allows us to evaluate the effects storage given changes in capacity, power rating, and distribution over the network using performance metrics such as cost and peak generation.

We extend the solution strategy described in [25] to an OPF problem formulation with simple storage dynamics. The procedure is based on solving a convex semi-definite program obtained as the Lagrangian dual to the rank relaxation of an equivalent reformulation for the OPF problem with storage dynamics. We show that under certain conditions, similar to those in [25], there is no duality gap between this reformulation and its Lagrangian dual. We then construct a solution for the reformulation (consequently for the OPF problem with storage dynamics) from that of the

This work was partially supported by the Boeing Corporation and AFOSR (FA9550-08-1-0043).

Department of Computing and Mathematical Sciences, California Institute of Technology, Pasadena, CA, USA, 91125. {dennice, utopcu}@cds.caltech.edu

dual problem. As an initial step, we study a case where uncertainties due to fluctuations in demand or intermittency in generation are neglected and focus on the effects of storage on the generation costs and peak-shaving using the IEEE benchmark networks described in [27] as examples.

II. Problem setup

Consider a power network with n buses and $m \leq n$ generators. Define $\mathcal{N} := \{1,\ldots,n\}$ and $\mathcal{G} := \{1,\ldots,m\}$ as the set of indices of all buses and generator nodes, respectively. Let $Y \in \mathbb{C}^{n\times n}$ be the admittance matrix defining the underlying network topology as described in [15], [28]. In the following, we extend an optimal power flow problem formulation from [15] to include simple dynamics for storage units located at each of the buses.

At generation buses $l \in \mathcal{G}$ and time $t = 1,\ldots,T$, the active power generation $P_l^g(t)$ and the reactive power generation $Q_l^g(t)$ are bounded as

$$P_l^{min} \leq P_l^g(t) \leq P_l^{max}, \tag{1a}$$

$$Q_l^{min} \leq Q_l^g(t) \leq Q_l^{max}. \tag{1b}$$

The magnitude of voltage $V_k(t)$ at bus $k \in \mathcal{N}$ at time $t = 1,\ldots,T$ is bounded as

$$V_k^{min} \leq |V_k(t)| \leq V_k^{max}. \tag{2}$$

At bus $k \in \mathcal{N}$, let $b_k(t)$ denote the amount of energy storage at time $t = 1,\ldots,T$ and $r_k(t)$ denote the rate of charge/discharge of energy at time $t = 1,\ldots,T-1$. The amount of storage at bus $k \in \mathcal{N}$ at time $t = 1,\ldots,T$ follows the first order difference equation[1]

$$b_k(t+1) = b_k(t) + r_k(t), \qquad \text{for } t = 1,\ldots,T-1, \tag{3}$$

with the initial condition

$$b_k(1) = \mathfrak{g}_k. \tag{4}$$

At each bus $k \in \mathcal{N}$, the amount $b_k(t)$ of storage and the rate $r_k(t)$ of charge/discharge are bounded as

$$0 \leq b_k(t) \leq B_k^{max}, \quad \text{for } t = 1,\ldots,T, \tag{5a}$$

$$R_k^{min} \leq r_k(t) \leq R_k^{max}, \quad \text{for } t = 1,\ldots,T-1. \tag{5b}$$

The network constraints at each $k \in \mathcal{N}$ and time $t = 1,\ldots,T$, can be expressed as

$$\begin{aligned} V_k(t)I_k^*(t) = P_k^g(t) - P_k^d(t) - r_k(t) \\ + \left[Q_k^g(t) - Q_k^d(t) - s_k(t)\right] \mathbf{i}. \end{aligned} \tag{6}$$

In (6), $s_k(t)$, the reactive part of the power flow in or out of the storage at bus $k \in \mathcal{N}$ and time $t = 1,\ldots,T$, is limited by

$$S_k^{min} \leq s_k(t) \leq S_k^{max}. \tag{7}$$

We use the convention that $P_k^g(t) = 0$ and $Q_k^g(t) = 0$ for $k \in \mathcal{N}\backslash\mathcal{G}$ and $t = 1,\ldots,T$ and $r_k(T) = 0$ and $s_k(T) = 0$ for $k \in \mathcal{N}$. Then, given the parameters in Table II, an optimal power flow problem with storage dynamics is written as

$$\begin{aligned} \varphi^* := \min \quad & \sum_{t=1}^{T}\sum_{l\in\mathcal{G}} c_{l2}(t)\left(P_l^g(t)\right)^2 + c_{l1}(t)P_l^g(t) \\ \text{subject to} \quad & \\ & (1),\ (2),\ (3),\ (4),\ (5),\ (6),\ \text{and}\ (7) \end{aligned} \tag{8}$$

over decision variables $V_j(t)$, $P_j^g(t)$, $Q_j^g(t)$, $b_j(t)$, $r_j(t)$, and $s_j(t)$ (with index j running over the sets indicated above).

Note that, in the conventional OPF formulation without storage, there is no correlation across time; therefore, the corresponding optimization is static and can be solved independently at each time. The admittance matrix indices optimization across the different generators. Storage allows optimization across time, i.e., charge when the cost of generation is low and discharge when it is high.

[1]With some abuse of notation $r_k(t)$ denotes the energy charged/discharged at storage at bus k over the period $[t, t+1]$.

TABLE I

Decision variables in optimization (8)

$P_k^g(t)$ and $Q_k^g(t)$	Real and reactive power generation at bus k and time t
$V_k(t)$	Complex voltage at bus k and time t
$b_k(t)$	Amount of storage at bus k and time t
$r_k(t)$	Real part of charge/discharge rate of storage at bus k and time t
$s_k(t)$	Imaginary part of charge/discharge rate of storage at bus k and time t

TABLE II

Parameters in optimization (8)

$P_k^d(t)$ and $Q_k^d(t)$	Real and reactive power demand at bus k and time t
P_l^{max}, P_l^{min}, Q_l^{max}, Q_l^{min}	Upper and lower bounds on real and reactive power generation at the generation bus l
V_k^{max}, V_k^{min}	Upper and lower bounds on voltage magnitude at bus k
B_k^{max}	Storage capacity at bus k
$\mathfrak{g}_k$	Initial storage at bus $k \in \mathcal{N}$
R_k^{max}, R_k^{min}	Upper and lower bounds on real rate of storage charge/discharge at bus k
S_k^{max}, S_k^{min}	Upper and lower bounds on reactive rate of storage charge/discharge at bus k
$Y \in \mathbb{C}^{n\times n}$	Admittance matrix

III. Solution strategy

The problem in (8) is non-convex in general. We now propose a convex relaxation of (8) and show that, under certain conditions, a solution to (8) can be constructed from that for this relaxation. To this end, we follow a similar procedure discussed in [25] and partly adopt their notation.

A. Reformulation of the OPF problem with storage

Let $e_k \in \mathbb{R}^n$, $k = 1,\ldots,n$, be the standard basis vectors for $\mathbb{R}^n$ and define

$$\begin{aligned} M_k &=: \mathrm{diag}(e_k e_k^*, e_k e_k^*), \\ Y_k &:= e_k e_k^* Y, \end{aligned}$$

$$\mathbf{Y}_k := \frac{1}{2}\begin{bmatrix} \text{Re}\left\{Y_k + Y_k^T\right\} & \text{Im}\left\{Y_k^T - Y_k\right\} \\ \text{Im}\left\{Y_k - Y_k^T\right\} & \text{Re}\left\{Y_k + Y_k^T\right\} \end{bmatrix},$$
$$\overline{\mathbf{Y}}_k := -\frac{1}{2}\begin{bmatrix} \text{Im}\left\{Y_k + Y_k^T\right\} & \text{Re}\left\{Y_k - Y_k^T\right\} \\ \text{Re}\left\{Y_k^T - Y_k\right\} & \text{Im}\left\{Y_k + Y_k^T\right\} \end{bmatrix},$$
$$U(t) := \left[\text{Re } V(t)^T \ \ \text{Im } V(t)^T\right]^T.$$

Note that

$$\text{Re}\{V_k(t)I_k^*(t)\} = \text{tr}\left\{\mathbf{Y}_k U(t)U^T(t)\right\}, \tag{9a}$$
$$\text{Im}\{V_k(t)I_k^*(t)\} = \text{tr}\left\{\overline{\mathbf{Y}}_k U(t)U^T(t)\right\}, \tag{9b}$$
$$|V_k(t)|^2 = \text{tr}\left\{M_k U(t)U^T(t)\right\}. \tag{9c}$$

By substituting

$$P_k^g(t) = \text{Re}\{V_k(t)I_k^*(t)\} + P_k^d(t) + r_k(t) \tag{10a}$$
$$Q_k^g(t) = \text{Im}\{V_k(t)I_k^*(t)\} + Q_k^d(t) + s_k(t) \tag{10b}$$

for $P_k^g(t)$, $Q_k^g(t)$ and then defining $W(t) := U(t)U(t)^T$, one can show that the problem in (8) is equivalent to the following optimization;

$$\varphi^* = \min_{W(t),\alpha(t),b(t),r(t),s(t)} \sum_{t=1}^{T}\sum_{l\in\mathcal{G}} \alpha_l(t) \tag{11}$$

subject to

$$P_k^{min} - P_k^d(t) \le \text{tr}\left\{\mathbf{Y}_k W(t)\right\} + r_k(t) \le P_k^{max} - P_k^d(t), \tag{12a}$$
$$Q_k^{min} - Q_k^d(t) \le \text{tr}\left\{\overline{\mathbf{Y}}_k W(t)\right\} + s_k(t) \le Q_k^{max} - Q_k^d(t), \tag{12b}$$
$$\left(V_k^{min}\right)^2 \le \text{tr}\left\{M_k W(t)\right\} \le \left(V_k^{max}\right)^2, \tag{12c}$$
$$0 \le b_k(t) \le B_k^{max}, \tag{12d}$$
$$R_k^{min} \le r_k(t) \le R_k^{max}, \tag{12e}$$
$$S_k^{min} \le s_k(t) \le S_k^{max}, \tag{12f}$$
$$b_k(t+1) = r_k(t) + b_k(t), \tag{12g}$$
$$b_k(1) = \mathfrak{g}_k, \tag{12h}$$
$$\begin{bmatrix} a_{l0}(t) & a_{l1}(t) \\ a_{l1}(t) & -1 \end{bmatrix} \preceq 0, \tag{12i}$$
$$W(t) \succeq 0, \tag{12j}$$
$$\text{rank}(W(t)) = 1, \tag{12k}$$

where

$$a_{l0}(t) := c_{l1}(t)\left[\text{tr}\left\{\mathbf{Y}_l W(t)\right\} + r_l(t) + P_l^d(t)\right] - \alpha_l(t),$$
$$a_{l1}(t) := \sqrt{c_{l2}(t)}\left[\text{tr}\left\{\mathbf{Y}_l W(t)\right\} + r_l(t) + P_l^d(t)\right].$$

As before, in (11)-(12), $k \in \mathcal{N}$, $l \in \mathcal{G}$ and time index $t = 1, \ldots, T$ except for (12g) where t runs over $\{1, \ldots, T-1\}$. Also $P_k^g(t) = 0$ and $Q_k^g(t) = 0$ for $k \in \mathcal{N}\backslash\mathcal{G}$ and $t = 1, \ldots, T$ with $r_k(T) = 0$ and $s_k(T) = 0$ for $k \in \mathcal{N}$. Note that constraint (12i) is equivalent to $c_{l2}(t)\left(P_l^g(t)\right)^2 + c_{l1}(t)P_l^g(t) \le \alpha_l(t)$ by the substitution in (10) and the Schur complement formula. The equivalence between (8) and (11)-(12) follows from the fact that a symmetric matrix $X \in \mathbb{R}^{n\times n}$ is positive semidefinite and of rank 1 if and only if there exists $x \in \mathbb{R}^n$ such that $X = xx^T$.

B. Lagrangian relaxation for the OPF problem with storage

We now develop a Lagrangian dual for optimization (11)-(12) excluding the rank constraints in (12k). To this end, let us introduce

$$z_l(t) := [z_{l0}(t), z_{l1}(t), z_{l2}(t)]^T, \quad l \in \mathcal{G},\, t \in \{1, \ldots, T\},$$

and

$$x(t) := \left[\lambda^{min}(t)^T,\, \lambda^{max}(t)^T,\, \eta^{min}(t)^T,\, \eta^{max}(t)^T,\, \mu^{min}(t)^T,\, \mu^{max}(t)^T,\, \gamma^{min}(t)^T,\, \gamma^{max}(t)^T,\, \rho^{min}(t)^T,\, \rho^{max}(t)^T,\, \xi^{min}(t)^T,\, \xi^{max}(t)^T\right]^T$$

and define

$$\begin{aligned} h(x,z,\sigma,\beta) := &-\sum_{t=1}^{T}\sum_{l\in\mathcal{G}} z_{l2}(t) - \sum_{k\in\mathcal{N}} \beta_k \mathfrak{g}_k \\ &+ \sum_{t=1}^{T}\sum_{k\in\mathcal{N}} \big\{\Lambda_k(t)P_k^d(t) + H_k(t)Q_k^d(t) \\ &+ \lambda_k^{min}(t)P_k^{min} - \lambda_k^{max}(t)P_k^{max} \\ &+ \eta_k^{min}(t)Q_k^{min} - \eta_k^{max}(t)Q_k^{max} \\ &+ \mu_k^{min}(t)\left(V_k^{min}\right)^2 - \mu_k^{max}(t)\left(V_k^{max}\right)^2 \\ &+ \rho_k^{min}(t)R_k^{min} - \rho_k^{max}(t)R_k^{max} \\ &- \gamma_k^{max}(t)B_k^{max} \\ &+ \xi_k^{min}(t)S_k^{min} - \xi_k^{max}(t)S_k^{max}\big\}, \end{aligned}$$

where

$$\Lambda_k(t) := \begin{cases} \lambda_k^{max}(t) - \lambda_k^{min}(t) \\ \qquad + c_{k1}(t) + 2\sqrt{c_{k2}(t)}z_{k1}(t), & k \in \mathcal{G}, \\ \lambda_k^{max}(t) - \lambda_k^{min}(t), & k \in \mathcal{N}\backslash\mathcal{G}, \end{cases}$$
$$H_k(t) := \eta_k^{max}(t) - \eta_k^{min}(t), \quad k \in \mathcal{N},$$
$$\Upsilon_k(t) := \mu_k^{max}(t) - \mu_k^{min}(t), \quad k \in \mathcal{N}$$

for $t \in \{0, \ldots, T\}$.

Consider the optimization

$$\psi^* := \max_{x\succeq 0, z,\sigma,\beta} h(x,z,\sigma,\beta) \tag{13}$$

subject to

$$\sum_{k\in\mathcal{N}} \left[\Lambda_k(t)\mathbf{Y}_k + H_k(t)\overline{\mathbf{Y}}_k + \Upsilon_k(t)M_k\right] \succeq 0, \tag{14a}$$
$$H_k(t) + \xi_k^{max}(t) - \xi_k^{min}(t) = 0, \tag{14b}$$
$$\Lambda_k(t) + \rho_k^{max}(t) - \rho_k^{min}(t) + \sigma_k(t+1) = 0, \tag{14c}$$
$$\sigma_k(t+1) - \sigma_k(t) + \gamma_k^{max}(t) - \gamma_k^{min}(t) = 0, \tag{14d}$$
$$\sigma_k(2) + \gamma_k^{max}(1) - \gamma_k^{min}(1) + \beta_k = 0, \tag{14e}$$
$$-\sigma_k(T) + \gamma_k^{max}(T) - \gamma_k^{min}(T) = 0, \tag{14f}$$
$$\begin{bmatrix} 1 & z_{l1}(t) \\ z_{l1}(t) & z_{l2}(t) \end{bmatrix} \succeq 0, \tag{14g}$$

where the indices k run over $\mathcal{N}$ and l over $\mathcal{G}$. The time index, $t = 1, \ldots, T$ in (14a), (14b) and (14g), $t = 1, \ldots, T-1$ in (14c), and $t = 2, \ldots, T-1$ in (14c) (14d).

Theorem 1: Optimization (13)-(14) is a Lagrangian dual of optimization (11)-(12) excluding the rank constraints in (12k) and strong duality holds.

Proof: Introduce the following correspondence between the constraints in (12) (all constraints on reals written as $f(y) \leq 0$ with $f : \mathbb{R}^\nu \to \mathbb{R}$ and all constraints on symmetric matrices written as $f(y) \preceq 0$ with $f : \mathbb{R}^\nu \to \mathbb{R}^{\omega \times \omega}$) and the decision variables in (13)-(14): $\lambda_k^{max}(t), \lambda_k^{min}(t) \geq 0$ for (12a); $\eta_k^{max}(t), \eta_k^{min}(t) \geq 0$ for (12b); $\mu_k^{max}(t), \mu_k^{min}(t) \geq 0$ for (12c); $\gamma_k^{max}(t), \gamma_k^{min}(t) \geq 0$ for (12d); $\rho_k^{max}(t), \rho_k^{min}(t) \geq 0$ for (12e); and $\xi_k^{max}(t), \xi_k^{min}(t) \geq 0$ for (12f) (in each case the variable with the superscript "max" ("min") corresponds to the upper (lower) bounds and the indices k and t run over the sets as indicated in (12)). For $k \in \mathcal{N}$ and $t = 1, \ldots, T-1$, $\sigma_k(t+1)$ corresponds to the constraint $b_k(t+1) = b_k(t) + r_k(t)$ in (12g) and β_k corresponds to that in (12h). Finally, let

$$\begin{bmatrix} z_{l0}(t) & z_{l1}(t) \\ z_{l1}(t) & z_{l2}(t) \end{bmatrix} \succeq 0$$

correspond to (12i) and $\Omega(t) \succeq 0$ correspond to (12j). Then, by standard manipulations on the Lagrangian (with the dual variables defined above), showing that $z_{l0}(t) = 1$ (through minimization of the Lagrangian with respect to $\alpha_l(t)$), and eliminating $\Omega(t)$, optimization (13)-(14) is a Lagrangian dual of (11)-(12) excluding the rank constraint in (12k). Note that both optimization problems (13)-(14) and (11)-(12) excluding the rank constraint in (12k) are convex. A strictly feasible solution can be constructed as follows:

$$\lambda_k^{min}(t) := \begin{cases} c_{k1}(t) + 1, & \text{for } k \in \mathcal{G} \\ 1, & \text{for } k \in \mathcal{N} \backslash \mathcal{G} \end{cases}$$

and for $k \in \mathcal{N}$, $\lambda_k^{max}(t) = 1$, $\eta_k^{max}(t) = \eta_k^{min}(t) = 1$, $\mu_k^{max}(t) = 2$, $\mu_k^{min}(t) = 1$, $\rho_k^{max}(t) = \rho_k^{min}(t) = 1$, $\gamma_k^{max}(t) = \gamma_k^{min}(t) = 1$ and $\xi_k^{max}(t) = \xi_k^{min}(t) = 1$, $\beta_k = 0$ when time indexes take values in $\{0, \ldots, T\}$ along with $z_{l0}(t) = 0$, $z_{l1}(t) = 1$ for $l \in \mathcal{G}$ and $t \in \{0, \ldots, T\}$, $\sigma_k(t+1) = 0$ for $k \in \mathcal{N}$ with time taking values in $\{0, \ldots, T-1\}$.

C. Constructing an optimal solution for the OPF problem with storage

Theorem 1 shows that there is no duality gap between optimization (13)-(14) and the rank relaxation of the (equivalent) reformulation of the OPF problem with storage in (11)-(12). In this section, we show, under certain assumptions, that there is no duality gap between the optimizations in (13)-(14) and (11)-(12).

Assumptions:

1) Optimization (11)-(12) is feasible and $W(t) = 0$ is infeasible for any $t \in \{1, \ldots, T\}$.
2) There exists an optimal solution to (13)-(14) with optimal values $(x^{opt}(t), z^{opt})$ for $(x(t), z(t))$ such that

$$A^{opt}(t) := \sum_{k=1}^{n} \left[\Lambda_k^{opt}(t) \mathbf{Y}_k + H_k^{opt}(t) \overline{\mathbf{Y}}_k + \Upsilon_k^{opt}(t) M_k \right]$$

has a zero eigenvalue of multiplicity two for $t = 1, \ldots, T$.

Remark 1: Assumption (1) is to avoid trivial solutions [25] and implies that $V(t) = 0$ is not feasible for (11)-(12) and equivalently for (8) for any t.

Remark 2: See [25] for a detailed discussion of assumption (2) and for its algebraic and geometric interpretations under the extra assumption that Y is symmetric with non-negative off-diagonal entries in $\text{Re}(Y)$ and nonpositive off-diagonal entries in $\text{Im}(Y)$.

Theorem 2: Under the assumptions (1) and (2) above, $\varphi^* = \psi^*$ and an optimal solution to (11)-(12) (and equivalently for (8)) can be constructed from that to (13)-(14).

The proof of Theorem 2 is a straightforward extension of a similar result in the case with no storage in [25, Theorem 1]. We now discuss the construction of an optimal solution to the OPF problem with storage. Let $[\nu_1(t)^T \; \nu_2(t)^T]^T$ be in the null space of $A^{opt}(t)$ with $\nu_1(t), \; \nu_2(t) \in \mathbb{R}^n$. Then, an optimal value $V^{opt}(t)$ for $V(t)$ can be computed as $V^{opt}(t) = (\zeta_1(t) + \zeta_2(t)\mathbf{i})(\nu_1(t) + \nu_2(t)\mathbf{i})$ where the constants $\zeta_1(t)$ and $\zeta_2(t)$ can be determined from the KKT conditions $\mu_k^{min}(t)((V_k^{min})^2 - |V_k(t)|^2) = 0$ and $\mu_k^{max}(t)(|V_k(t)|^2 - (V_k^{max})^2) = 0$ or the fact that the phase angle at the swing (reference) bus is known (e.g., zero). An optimal value of $W(t)$ can be computed through $W(t) = U(t)U(t)^T$. Then, optimal values for P^g, Q^g, b, r, and s are computed through the KKT conditions: for $k \in \mathcal{N}$,

$$\begin{aligned}
\lambda_k^{min}(t) \left[\text{tr}\{\mathbf{Y}_k W(t)\} + r_k(t) - P_k^{min} + P_k^d(t) \right] &= 0, \\
\lambda_k^{max}(t) \left[P_k^{max} - P_k^d(t) - \text{tr}\{\mathbf{Y}_k W(t)\} - r_k(t) \right] &= 0, \\
\eta_k^{min}(t) \left[\text{tr}\{\overline{\mathbf{Y}}_k W(t)\} + s_k(t) - Q_k^{min} + Q_k^d(t) \right] &= 0, \\
\eta_k^{max}(t) \left[Q_k^{max} - Q_k^d(t) - \text{tr}\{\overline{\mathbf{Y}}_k W(t)\} - s_k(t) \right] &= 0, \\
\gamma_k^{min}(t) b_k(t) = 0, \qquad \gamma_k^{max}(t) \left[B_k^{max} - b_k(t) \right] &= 0,
\end{aligned}$$

for $t = 1, \ldots, T$,

$$\begin{aligned}
\rho_k^{min}(t) \left[r_k(t) - R_k^{min} \right] = 0, \quad \rho_k^{max}(t) \left[R_k^{max} - r_k(t) \right] &= 0, \\
\xi_k^{min}(t) \left[s_k(t) - S_k^{min} \right] = 0, \quad \xi_k^{max}(t) \left[S_k^{max} - s_k(t) \right] &= 0, \\
\sigma_k(t+1) \left[r_k(t) - b_k(t+1) + b_k(t) \right] &= 0,
\end{aligned}$$

for $t = 1, \ldots, T-1$, and $\beta_k \left[b_k(1) - \mathfrak{g}_k \right] = 0$ and the conditions in (10).

IV. Examples

In this section, we illustrate the effect of energy storage using the IEEE 14 bus benchmark example [27] with different cost functions of the form (8). This benchmark system, which represents a portion of the Midwestern US Electric Power System as of February, 1962 [27], does not include storage. Therefore, while we use its network topology as well as its voltage and generation bounds, (i.e., V^{max}, V^{min}, P^{max}, P^{min}, Q^{max} and Q^{min} in (2) and (1)), we need to add appropriate values for the storage parameters as well as time-varying demand profiles. We created demand profiles for each bus using typical hourly demands for 14 different 2009 December days in Long Beach, CA, USA

[29]. The curves are scaled so that their peak corresponds to the static demand values in the IEEE 14 bus test case. Figure 1 shows the demand curves for each bus. For all of the results presented here the rate limits in (5) are set to $R_k^{max} = 8$ and $R_k^{min} = -8$ Mega Watts (MW) for each bus. The reactive rate limits (S_k^{max} and S_k^{min} in (7)) are set to keep the rate angle between $-18\,\deg$ and $48\,\deg$. This range was selected based on the real and reactive generation limits in the IEEE 14 bus test case which give rise to generator angles approximately between $-17\,\deg$ and $90\,\deg$. Unless otherwise indicated all power values reported in the following sections are normalized to per unit values (p.u.) as described in [15].

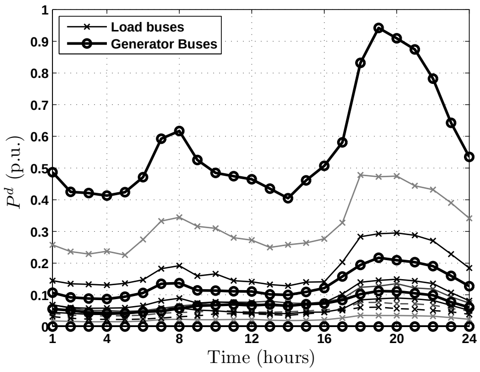

Fig. 1. Hourly demands peak scaled to match the demands in IEEE 14 bus benchmark case. The load profiles represent demands for 14 different typical days in December 2009 in Long Beach, CA, USA.

A. Example I: Linear cost

We first use a cost function that is the sum of the total generation (i.e., $\|P^g\|_1 = \sum_{t=1}^{T} \sum_{l \in \mathcal{G}} P_l^g(t)$) and refer to this as a time-invariant linear cost function since the coefficients $c_{l1}(t) = 1$ and $c_{l2}(t) = 0$ from (8) are constant in time for each $l \in \mathcal{G}$. Figure 2 shows that the addition of storage (32 MWh per bus) as well as the finite-time optimization horizon produces a flatter generation curve over the time period. This change is most evident for generators 4 and 5 (respectively P_4^g and P_5^g). For this cost function generator 1 is not used. A constant generation profile is desirable from an operator perspective as the efficiency of most of the conventional generators are optimized for full capacity. As a result, many operators maintain generation levels that will accommodate the peak demand which can lead to excess power being curtailed.

There has been a great deal of research aimed at demand based pricing strategies, (i.e., higher prices at peak demand times). The thick black line on the top panel of Figure 4 shows that the average demand begins to increase around $t = 15$. In order to simulate this affect we use a weighed ℓ_1 norm (i.e., $\sum_{t=1}^{T} \sum_{l \in \mathcal{G}} c_{l1}(t) P_l^g(t)$) for the cost function in (8) where for each generator $l \in \mathcal{G}$ the parameter $c_{l1}(t) = 1$ for $t \in \{1, \ldots 15\}$ and $c_{l1}(t) = 1.5$ for $t \in \{16, \ldots 24\}$ and refer to this case as the time-varying cost function. Figure 2 shows that this time-varying cost function further regulates the

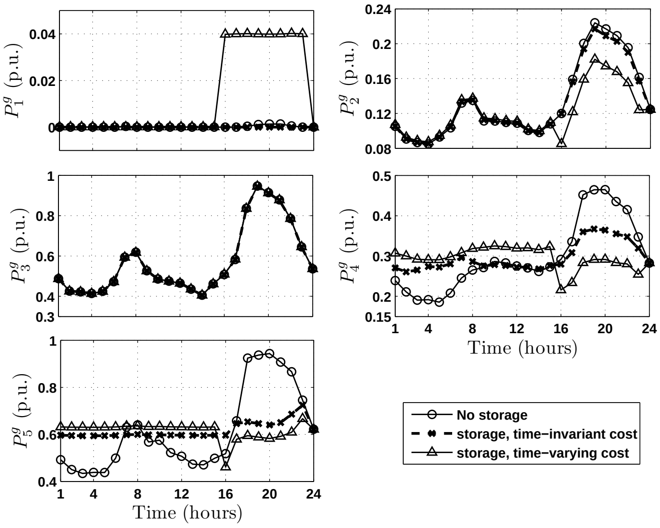

Fig. 2. Hourly generation for each $l \in \mathcal{G}$. The addition of 32 MWh storage at each bus as well as optimization over time results in flatter generation profiles, especially when a demand based time-varying cost function is used. This smoothing of the generation curve is most evident for generators 4 and 5. Generators 2 and 3 produce power primarily to track their own load.

demand profile to an essentially constant level for generators 4 and 5 and reduces the peak-to-trough spread on generator 2. Some of the demand is also satisfied by requiring a small amount of generation from generator 1 during the peak period. It should be noted that generators 2 and 3 produce power primarily to track their own load, for both the time-invariant and time-varying linear cost functions. One reason that the finite-time horizon optimization with storage does not flatten all of the generation profiles is because the linear cost function (i.e., ℓ_1 norm based) only attempts to minimize overall generation rather than the total energy of the power signal.

The left panel of Figure 3 shows how the value of both time-invariant and time-varying cost functions (normalized such that each $P_l^g(t)$ for $l \in \mathcal{G}$ and $t \in \{0, \ldots T\}$ is a p.u. value) change with the amount of per bus storage capacity B^{max} in MWh. For time-independent costs, the storage reduces the cost (which is equivalent to total generation) by a small percent. However, a simple demand based cost structure increases the cost benefit by about 2% for a doubling of storage capacity.

B. Example II: Quadratic cost

In this subsection, we repeat the computations described in section IV-A for both time-invariant and time-varying quadratic cost functions. Again, we use the peak normalized demand profiles shown in the top panel of Figure 4 to determine that $t = 15$ is the time step where the average demand starts to increase toward peak levels. The higher cost function coefficients for $t \geq 15$ are thus meant to reflect a demand based pricing scheme. We obtain the second order coefficients directly from the IEEE 14 bus test case. The linear coefficients were selected to maintain the ratio of costs between the generators in the test case. For the time-invariant

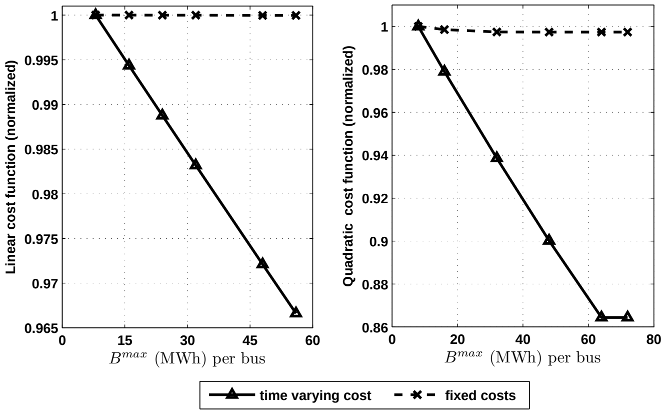

Fig. 3. Cost versus per bus storage capacity (B^{max} in MWh) at each bus. The left panel is for a linear cost function and the right panel for a quadratic cost function. The cost always decreases with increased storage capacity. For time-varying coefficients the decrease in cost is roughly linear as a function of per bus storage capacity for both cost functions.

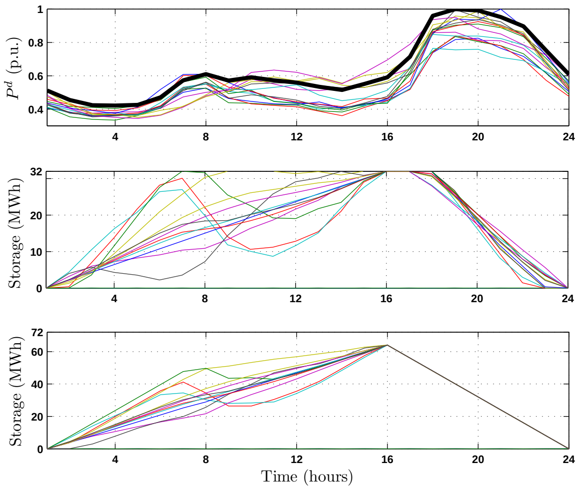

Fig. 4. The top panel shows the peak normalized demand. At $t = 15$ the average demand (shown as the thick line and excluding buses with no demand) starts to increase toward peak levels, this defines the point where the cost function coefficients are increased to reflect a demand based pricing scheme. The center and lower panels respectively show the storage use for the time-varying quadratic cost function based on per bus capacity constraints of 32 and 72 MWh respectively. For the higher storage capacity the full capacity is never used.

case the coefficients for $t = 1, \ldots, 24$, are; $c_{12}(t) = 0.043$, $c_{22}(t) = 0.250$, $c_{l2} = 0.01$ for $l = 3, 4, 5$, $c_{l1}(t) = 2$ for $l = 1, 2$, and $c_{l1}(t) = 4$ and $c_{l2}(t) = 0.010$ for $l = 3, 4, 5$. For the time-varying case the quadratic term coefficients, $c_{l2}(t)$ for $l \in \{1, \ldots, 5\}$ and for all t, are the same as in the time-independent case. The first order coefficients $c_{l1}(t) = 2$ for $l = 1, 2$ and $c_{l1}(t) = 4$ for $l = 3, 4, 5$ for $t = 1, \ldots, 15$, and $c_{l1}(t) = 4$ for $l = 1, 2$ and $c_{l1}(t) = 8$ for $l = 3, 4, 5$ for $t = 16, \ldots, 24$,. The right panel in Figure 3 indicates that, as with the linear cost function, the cost decreases approximately linearly with storage but the slope is significantly steeper with roughly a 4% decrease with a doubling of per bus storage capacity until we reach a limit beyond which additional storage no longer affects the cost.

Figure 4 shows the relationship between storage use and demand for the time-varying quadratic cost function. The top panel reflects peak normalized demand at each bus. The average per bus demand (excluding buses with no demand) is superimposed on the rest of the curves with a thick black line. The center and lower panels reflect the storage use with two different per bus capacity constraints (respectively, $B^{max} = 32$ MWh and $B^{max} = 72$ MWh). As the demand increases the storage is charged until the time increment before the first local peak (at $t = 8$), then the storage is used to reduce the generation load until the demand stabilizes. Finally the storage is recharged until the peak load and then discharged until the end of the day. For the higher storage capacity constraint ($B^{max} = 72$ MWh) the storage is never fully charged. The maximum usage occurs at approximately 64 MWh, which explains why the cost function value does not change for the last two points (per bus B^{max} levels) on the right panel of Figure 3.

Figure 5 shows that a quadratic time-varying cost function along with storage further flattens the generation profiles. For the quadratic time-varying costs generators 1 and 2 provide all of the required power. Clearly, the form of the cost function favors the use of the first two generators. The addition of storage and an optimization over time produces almost constant levels of generation for generator 1 over the 24 hour period when compared to the no storage case. For generator 2, the range is reduced from $[0.24, 0.71]$ to $[0.30, 0.54]$.

Remark 3: It was observed in [25] that Assumption (2) in section III-C is satisfied in many of the IEEE benchmark systems when a small amount of resistance (e.g., of the order of 10^{-5} per unit) was added to each transformer. In the numerical examples in this paper, we implement this modification. This modification essentially renders the graph induced by $\mathrm{Re}(Y)$ strongly connected.

V. Summary and Potential Extensions

We formulated an optimal power flow problem with simple charge/discharge dynamics for energy storage collocated with load and/or generation buses as a finite-time optimal control problem. The resulting optimization problem, under certain conditions (discussed in the previous sections), was solved using a procedure based on a convex semi-definite program obtained as a Lagrangian dual to the rank relaxation of an equivalent formulations for the OPF problem with storage dynamics. We investigated effects of storage capacity and power rating on generation costs and peak reductions using a modified version of the IEEE 14 benchmark system which represents a portion of the Midwestern U.S. Electric Power System.

As discussed in the earlier sections, the motivation of the current work is to assess the utility of grid-integrated storage

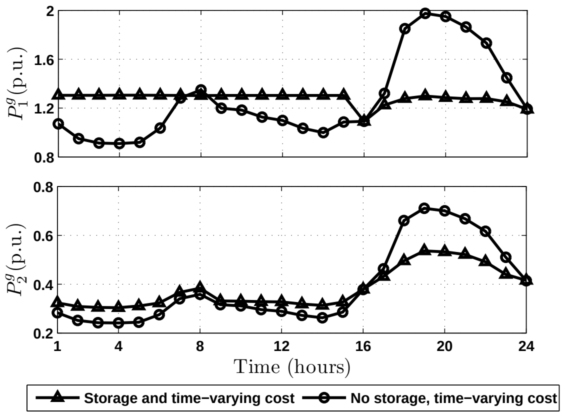

Fig. 5. Generation comparison for storage ($B^{max} = 32$ MWh per bus) and no storage with quadratic time-varying cost functions. Generators 3–5 do not generate power for either scenario.

in mitigating issues associated with integration of intermittent renewable energy resources into the electric power grid. As a step toward this goal, the current paper focused on a case with no uncertainties. Integration of uncertainties due to either intermittency in generation or fluctuations in demand is a subject of ongoing study. Another natural extension is assessing effects of the distribution of energy storage systems in the power grid to minimize losses and defer the expansion requirements of transmission capacities.

The role of energy storage is to provide flexibility to the power systems for dealing with a number of concerns including power quality, stability, load following, peak reduction, and reliability. A promising direction is assessing the suitability of hybrid storage technologies (e.g., a combination of pumped-hydro, thermal, and batteries) in addressing these issues. Additionally, similar flexibility can be acquired through spinning reserves and/or conventional generators with high ramp rates. An interesting design issue is deciding on an appropriate balance between the storage and ancillary generation capacities.

ACKNOWLEDGEMENTS

The authors gratefully acknowledge George Rodriguez and Christopher Clarke of Southern California Edison as well as Mani Chandy of the California Institute of Technology for fruitful discussions and helpful suggestions.

REFERENCES

[1] T. Ackerman, Ed., *Wind Power in Power Systems*. Wiley, 2005.
[2] J. Carrasco, L. Franquelo, J. Bialasiewicz, E. Galván, R. P. Guisado, M. M. Prats, J. León, and N. Moreno-Alfonso, "Power-electronic systems for the grid integration of renewable energy sources: A survey," *IEEE Trans. Industrial Electronics*, vol. 53, no. 4, pp. 1002–1016, 2006.
[3] V. Budhraja, F. Mobasheri, M. Cheng, J. Dyer, E. Castano, S. Hess, and J. Eto, "California's electricity generation and transmission interconnection needs under alternative scenarios," California Energy Commission, Tech. Rep., 2004.
[4] "Annual energy outlooks 2010 with projections to 2035," U.S. Department of Energy, Energy Information Administration, Tech. Rep. DOE/EIA-0383, 2010. [Online]. Available: http://www.eia.doe.gov/oiaf/aeo
[5] J. P. Barton and D. G. Infield, "Energy storage and its use with intermittent renewable energy," *IEEE Trans. Energy Conversion*, vol. 19, no. 2, pp. 441–448, 2004.
[6] S. M. Schoenung, J. M. Eyer, J. J. Iannucci, and S. A. Horgan, "Energy storage for a competitive power market," *Annual Review of Energy and the Environment*, vol. 21, no. 1, pp. 347–370, 1996.
[7] R. Schainker, "Executive overview: Energy storage options for a sustainable energy future," in *Proc. IEEE Power Eng. Soc. General Meeting*, 2004, pp. 2309–2314.
[8] J. W. Tester, E. M. Drake, M. J. Driscoll, M. W. Golay, and W. A. Peters, *Sustainable Energy: Choosing Among Options*. MIT Press, 2005.
[9] T. Yau, L. Walker, H. Graham, and A. Gupta, "Effects of battery storage devices on power system dispatch," *IEEE Trans. Power Apparatus and Sys.*, vol. PAS-100, no. 1, pp. 375–383, 1981.
[10] N. Alguacil and A. J. Conejo, "Multiperiod optimal power flow using benders decomposition," *IEEE Trans. Power Sys.*, vol. 15, no. 1, pp. 196 –201, 2000.
[11] M. Geidl and G. Andersson, "A modeling and optimization approach for multiple energy carrier power flow," in *In Proc. of IEEE PES PowerTech*, 2005.
[12] E. Sortomme and M. A. El-Sharkawi, "Optimal power flow for a system of microgrids with controllable loads and battery storage," in *Power Sys. Conf. and Exposition*, 2009.
[13] Y. M. Atwa and E. F. El-Saadany, "Optimal allocation of ESS in distribution systems with a high penetration of wind energy," *IEEE Trans. Power Sys., to appear*, 2010.
[14] H. Xu, U. Topcu, S. Low, and M. Chandy, "On load-shedding probabilities of power systems with renewable power generation and energy storage," in *Proc. Allerton Conf. on Communication, Control and Computing*, 2010.
[15] J. A. Momoh, *Electric Power System Applications of Optimization*, ser. Power Engineering, H. L. Willis, Ed. Markel Dekker Inc.: New York, USA, 2001.
[16] W. W. Hogan, "Contract networks for electric power transmission," *J. of Regulatory Economics*, vol. 4, no. 3, pp. 211–42, 1992.
[17] H. P. Chao and S. Peck, "A market mechanism for electric power transmission," *J. of Regulatory Economics*, vol. 10, pp. 25–59, 1996.
[18] H. P. Chao, S. Peck, S. Oren, and R. Wilson, "Flow-based transmission rights and congestion management," *The Electricity J.*, vol. 13, no. 8, pp. 38–58, 2000.
[19] J. Carpentier, "Contribution to the economic dispatch problem," *Bulletin de la Societe Francoise des Electriciens*, vol. 3, no. 8, pp. 431–447, 1962, in French.
[20] M. Huneault and F. D. Galiana, "A survey of the optimal power flow literature," *IEEE Trans. Power Sys.*, vol. 6, no. 2, pp. 762–770, 1991.
[21] J. A. Momoh, M. E. El-Hawary, and R. Adapa, "A review of selected optimal power flow literature to 1993, part I: Nonlinear and quadratic programming approaches," *IEEE Trans. Power Sys.*, vol. 14, no. 1, pp. 96–104, 1999.
[22] K. S. Pandya and S. K. Joshi, "A survey of optimal power flow methods," *J. of Theoretical and Applied Information Technology*, vol. 4, no. 5, pp. 450–458, 2008.
[23] R. A. Jabr, "Radial distribution load flow using conic programming," *IEEE Trans. Power Sys.*, vol. 21, no. 3, pp. 1458–1459, 2006.
[24] ——, "Optimal power flow using an extended conic quadratic formulation," *IEEE Trans. Power Sys.*, vol. 23, no. 3, pp. 1000–1008, 2008.
[25] J. Lavaei and S. Low, "Convexification of optimal power flow problem," in *Proc. Allerton Conf. on Communication, Control and Computing*, 2010.
[26] M. Chandy, S. Low, U. Topcu, and H. Xu, "A simple optimal power flow model with energy storage," in *Proc. Conf. on Decision and Control*, 2010.
[27] University of Washington, "Power systems test case archive." [Online]. Available: http://www.ee.washington.edu/research/pstca/
[28] R. D. Zimmerman, C. E. Murillo-Sánchez, and R. J. Thomas, "MATPOWER's extensible optimal power flow architecture," in *Proc. IEEE Power Eng. Soc. General Meeting*, 2009, pp. 1–7.
[29] Personal communication with researchers from Southern California Edison.